NeuroImage 266 (2023) 119807

Contents lists available at ScienceDirect

NeuroImage

journal homepage: www.elsevier.com/locate/neuroimage

BrainStat: A toolbox for brain-wide statistics and multimodal feature associations

Sara Larivière[a,1], Şeyma Bayrak[b,1], Reinder Vos de Wael[a,1], Oualid Benkarim[a], Peer Herholz[a], Raul Rodriguez-Cruces[a], Casey Paquola[c], Seok-Jun Hong[d,e], Bratislav Misic[a], Alan C. Evans[a], Sofie L. Valk[b,c], Boris C. Bernhardt[a,*]

[a] McConnell Brain Imaging Centre, Montreal Neurological Institute, McGill University, Montreal, Quebec, Canada
[b] Max Planck Institute for Human Cognitive and Brain Sciences, Leipzig, Germany
[c] Institute of Neuroscience and Medicine (INM-1), Forschungszentrum Jülich, Germany
[d] Child Mind Institute, New York, USA
[e] Center for Neuroscience Imaging Research, Institute for Basic Science, and Department of Biomedical Engineering, Sungkyunkwan University, Suwon, South Korea

ARTICLE INFO

Keywords:
Neuroimaging
Multivariate analysis
Univariate analysis

ABSTRACT

Analysis and interpretation of neuroimaging datasets has become a multidisciplinary endeavor, relying not only on statistical methods, but increasingly on associations with respect to other brain-derived features such as gene expression, histological data, and functional as well as cognitive architectures. Here, we introduce BrainStat - a toolbox for *(i)* univariate and multivariate linear models in volumetric and surface-based brain imaging datasets, and *(ii)* multidomain feature association of results with respect to spatial maps of *post-mortem* gene expression and histology, task-based fMRI meta-analysis, as well as resting-state fMRI motifs across several common surface templates. The combination of statistics and feature associations into a turnkey toolbox streamlines analytical processes and accelerates cross-modal research. The toolbox is implemented in both Python and MATLAB, two widely used programming languages in the neuroimaging and neuroinformatics communities. BrainStat is openly available and complemented by an expandable documentation.

1. Introduction

Neuroimaging enables brain-wide measures of morphology, microstructure, function, and connectivity in individuals as well as large cohorts (Casey et al., 2018; Glasser et al., 2013; Royer et al., 2021). Through an increasing array of powerful image processing techniques (Cameron et al., 2013; Esteban et al., 2019; Fischl, 2012; Kim et al., 2005), these data can be brought into a standardized frame of reference including stereotaxic voxel spaces such as the commonly used MNI152 space (Collins et al., 2003; Dadar et al., 2018), surface-based spaces such as fsaverage, MNI152-CIVET surfaces, or grayordinates (Fischl, 2012; Glasser et al., 2013; Kim et al., 2005; Lyttelton et al., 2007; Marcus et al., 2011), as well as parcellation schemes (Desikan et al., 2006; Glasser et al., 2016; Gordon et al., 2016; Schaefer et al., 2017). Registering neuroimaging data to a common space allows for the application of statistical analyses, including mass-univariate generalized linear and mixed-effects models that carry out parallel statistical tests at each measurement unit. Usually, such analyses need to be carried out using multiple tools and programs, reducing the reproducibility of workflows, and increasing the risk of human error. With the current paper, we present BrainStat, a unified toolbox to implement these analyses in a cohesive, transparent, and open-source framework.

Advanced analytical workflows of neuroimaging studies increasingly rely on the availability of previously acquired datasets across multiple (non)imaging modalities. When mapped to the same reference frame as the neuroimaging measures, these datasets can be used for contextualization of findings and aid in interpretation and validation of results. For example, results may be contextualized within established motifs of the brain's functional architecture such as intrinsic functional communities based on resting-state fMRI (Yeo et al., 2011) or functional gradients (Margulies et al., 2016), both allowing for the interpretation of findings based on the established brain's functional architecture. Another common method for contextualization is automated meta-analysis with Neurosynth (Yarkoni et al., 2011), NiMARE (Salo et al., 2020), or BrainMap (Laird et al., 2005). These tools offer the ability to carry out *ad hoc* meta-analyses across potentially thousands of previously published fMRI studies. Correlating a statistical map with a database of brain activation maps related to cognitive terms, so-called meta-analytical decod-

* Corresponding authors at: Montreal Neurological Institute, McGill University, Montreal, QC, Canada.
E-mail addresses: valk@cbs.mpg.de (S.L. Valk), boris.bernhardt@gmail.com (B.C. Bernhardt).
[1] Equal contributions

https://doi.org/10.1016/j.neuroimage.2022.119807.
Received 25 May 2022; Received in revised form 28 November 2022; Accepted 9 December 2022
Available online 10 December 2022.

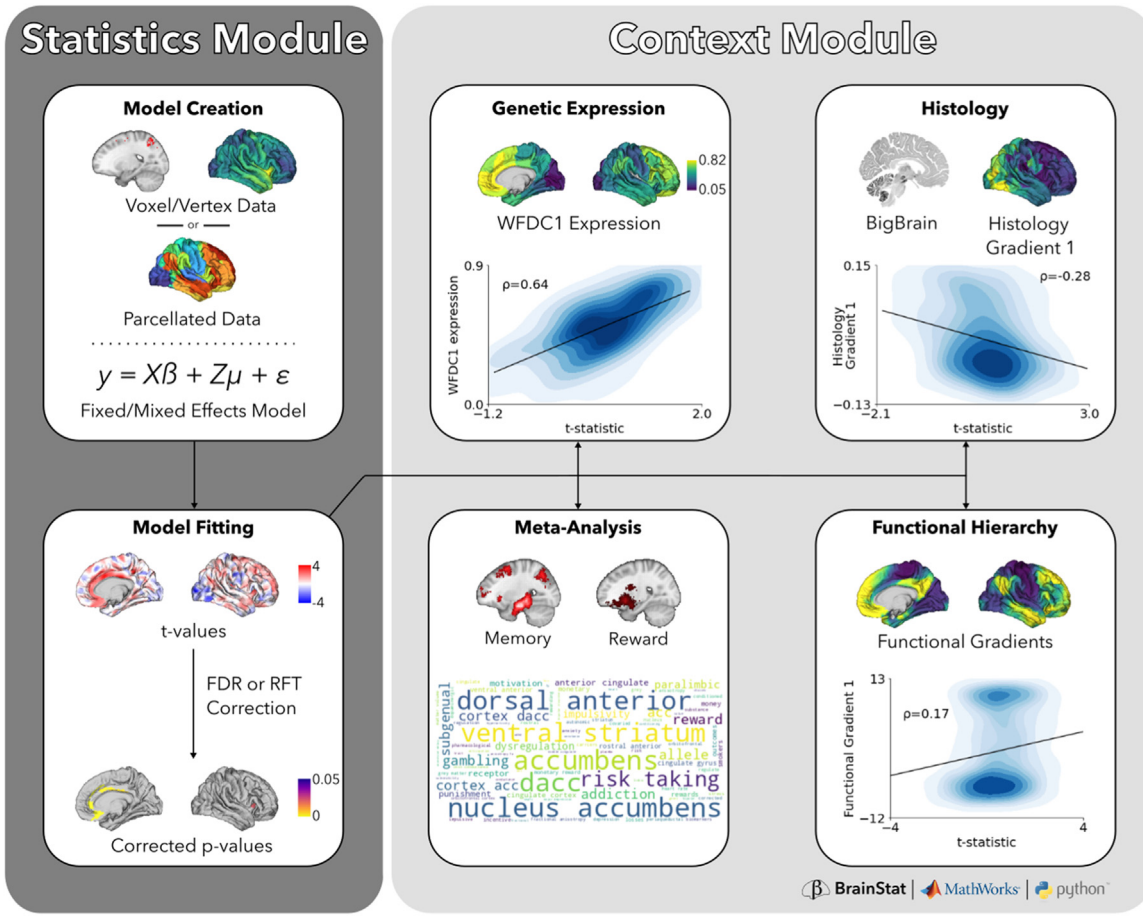

Fig. 1. BrainStat workflow. The workflow is split into a statistics module (dark grey) for linear fixed and mixed effects models and a context module (light grey) for contextualizing results with external datasets. To use the statistics module, the user must provide voxel-, vertex-, or parcel-wise data, must specify a fixed or mixed effects model, and must specify a model contrast. Once these have been specified, BrainStat computes *t*-values and corrected *p*-values for the model. *t*-value maps, or any other brain map, can then be used in the context module to embed the statistical results with markers of task fMRI meta-analyses and established functional hierarchies, genetic expression, and histological markers.

ing, offers a quantitative approach to infer plausible cognitive processes related to a spatial statistical pattern. Finally, *post-mortem* datasets of transcriptomics (Hawrylycz et al., 2012) and histology (Amunts et al., 2013) mapped to a common neuroimaging space enable associations of neuroimaging findings with gene expression and microstructural patterns (Markello et al., 2021; Paquola et al., 2021). Such findings can provide information on molecular and cellular properties in the brain that spatially co-vary with an observed statistical map. By combining these feature association techniques, the functional, histological, and genetic correlates of neuroimaging findings can be inferred. BrainStat provides an integrated decoding engine to perform these multimodal feature associations.

Our toolbox has a parallel implemented in both Python and MATLAB, two common programming languages in the neuroimaging research community. One key design choice of BrainStat was, thus, to aim for maximally homogenized implementations, which enhance accessibility of the tool and help users aiming to learn one or both programming languages without a priori programming expertise. BrainStat relies on a simple object-oriented framework to streamline the analysis workflow. The toolbox is openly available at https://github.com/MICA-MNI/BrainStat with documentation available at https://brainstat.readthedocs.io/. We have compartmentalized the toolbox into two main modules: statistics and contextualization (Fig. 1). In the remainder of this manuscript, we describe how to perform the analyses shown in Fig. 1.

2. Statistics module

The statistics module was built upon SurfStat, a classic but non-maintained MATLAB package for the implementation of fixed and mixed effects linear models (Worsley et al., 2009). To create and fit such a model in the BrainStat implementation, the user provides a subject-by-region-by-variate response matrix as well as a predictor model, created using an intuitive model formula framework. This approach allows for a straightforward definition of fixed/random effects as variables of main interest or control covariates, facilitating both cross-sectional as well as longitudinal analyses. For mixed effects modelling, BrainStat uses a G-side specification, such that it can accommodate multiple random effects as independent effects, with the fitting currently being done via restricted maximum likelihood estimation.

To compare the effects of variables of interest (*e.g.*, healthy/disease, age), a contrast must be specified. BrainStat can handle either univariate or multivariate response data and provides two widely used analytical options for multiple comparison corrections, namely false discovery rate (Benjamini & Hochberg, 1995) and random field theory (Worsley et al., 1999). False discovery rate controls the proportion of pointwise (*i.e.*, vertex, voxel, parcel) false positives in the data, whereas random field theory corrects for the probability of ever reporting a false positive finding (either at the peak or cluster level).

To illustrate the statistics module, we downloaded cortical thickness and demographic data of 70 participants, 12 of whom were

A

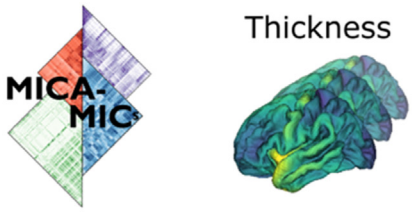

Demographics

SUB_ID	VISIT	AGE_AT_SCAN	SEX
'04A144'	1	-0.8121159	'M'
'0D26B9'	1	0.4662934	'F'
'26899F'	1	-0.9283349	'M'
'26899F'	2	-0.6958969	'M'

B

```
from brainstat.datasets import fetch_mask
from brainstat.stats.SLM import SLM
from brainstat.stats.terms import FixedEffect, MixedEffect
from brainstat.tutorial.utils import fetch_mics_data

thickness, demographics = fetch_mics_data()
mask = fetch_mask("fsaverage5")

term_age = FixedEffect(demographics.AGE_AT_SCAN)
term_sex = FixedEffect(demographics.SEX)
term_subject = MixedEffect(demographics.SUB_ID)
model = term_age + term_sex + term_age * term_sex + term_subject

contrast_age = -demographics.AGE_AT_SCAN
slm = SLM(
    model,
    contrast_age,
    surf="fsaverage5",
    mask=mask,
    correction=["fdr", "rft"],
    cluster_threshold=0.01,
)
slm.fit(thickness)
```

C

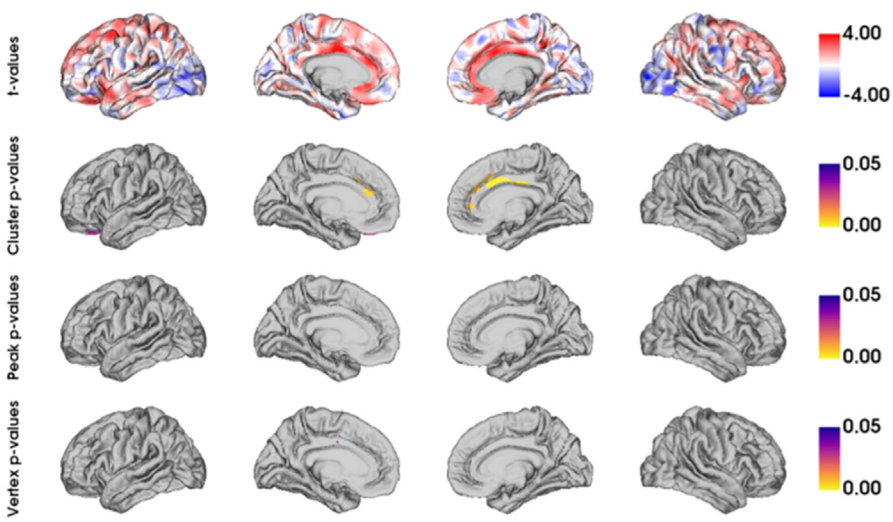

Fig. 2. Example Python code for fitting a fixed effect general linear model of the effect of age on cortical thickness with BrainStat. (A) The MICA-MICS dataset included with BrainStat contains cortical thickness and demographics data. The demographics data contain hashed subject IDs (SUB_ID), visit number (VISIT), *z*-scored age on the day of scanning (AGE_AT_SCAN), and sex (SEX). (B) We create a linear model in the form of $\boldsymbol{Y = intercept + age + sex + age * sex + random(subject)}$. Note that the intercept is included in the model by default. Third, we initialize the model with an age contrast and request both *p*-values corrected with random field theory (*i.e.*, "rft") as well as those corrected for false discovery rate (*i.e.*, "fdr"). Lastly, we fit the model to the cortical thickness data. (C) Negative t-values (blue) indicate decreasing cortical thickness with age, whereas positive t-values (red) depict increasing cortical thickness with age. Significant peak-wise and cluster-wise p-values ($p<0.05$) are shown for a random field theory (RFT) correction (cluster defining threshold $p<0.01$) as well as vertex-wise p-values ($p<0.05$) derived with false discovery rate (FDR) correction. Figure plotting code was omitted for brevity. Python and MATLAB code for this model, as well as code for plotting these figures can be found in the supplemental Jupyter notebook and live script.

scanned twice, of the Microstructure-Informed Connectomics (MICA-MICs) dataset (Royer et al., 2021) (Fig. 2**A**). We created a linear model with age and sex as well as their interaction effect as fixed effects, and subject as a random effect (Fig. 2**B**). These are set up using the FixedEffect and MixedEffect (named as such as it may contain both random and fixed effects) classes. Next, we defined the contrast as –age, i.e., positive *t*-values denote decreasing cortical thickness with age. This model was fitted on cortical thickness data using a one-tailed test. The *t*-values, cluster-wise and peak *p*-values derived from random field theory, as well as the vertex-wise *p*-values derived with a correction for false discovery rate were plotted in Fig. 2**C**. We found that, in the MICA-MICs dataset, there is an effect of age on cortical thickness at the cluster level based

on random-field theory, but no significant vertex-wise peaks within these clusters, and marginal significance at a vertex-level. This suggests that the effect of age on cortical thickness covers broad regions, rather than local foci. Although we used a liberal cluster-defining threshold ($p<0.01$) for this illustration, we generally recommend a more stringent threshold ($p<0.001$), particularly if data with little spatial smoothing are used (Eklund et al., 2016; Woo et al., 2014).

The quality and robustness of any fitted model can be assessed at every vertex/parcel on the cortex, for a specific vertex/parcel, or for a combination of vertices/parcels. To test for normality of the data, our quality control function outputs a histogram of the residuals and a q-q plot of the residuals versus the theoretical quantile values from a normal distribution. Vertex- or parcelwise measures of skewness and kurtosis, characterizing the residual distributions across the cortex, are also mapped onto the brain surface.

3. Context module

The context module enables the calculation of bivariate correlations of statistical maps with multimodal neural features. As of version 0.3.6, the context module can link to: (*i*) *in vivo* task-based fMRI meta-analysis, (*ii*) *in-vivo* functional motifs derived from resting-state fMRI, (*iii*) *post mortem* genetic expression, and (*iv*) *post mortem* histology/cytoarchitecture (Fig. 1). The meta-analysis submodule tests for associations between brain maps and task-fMRI meta-analyses associated with particular terms (Salo et al., 2020; Yarkoni et al., 2011). The resting-state module contextualizes neuroimaging findings relative to functional gradients (Margulies et al., 2016; Vos de Wael et al., 2020), a low-dimensional approach to represent the functional connectome. The transcriptomics submodule extracts gene expression from the Allen Human Brain Atlas (Hawrylycz et al., 2012). Lastly, the histological submodule fetches cell-body-staining intensity profiles from the BigBrain (Paquola et al., 2021), a 3D reconstruction of human brain cytoarchitecture (Amunts et al., 2013). These submodules all support common surface templates and, wherever feasible, custom parcellations. Collectively, they pave the way for enrichment analysis of statistical results with respect to aspects of micro- and macroscale brain organization.

3.1. Meta-analytic decoding

The meta-analytic decoding submodule of BrainStat uses data derived from Neurosynth and NiMARE (Salo et al., 2020; Yarkoni et al., 2011; Salo et al., 2018) to decode a statistical map in terms of its cognitive associations (derived via meta-analyses of prior task-based functional MRI findings). In short, a meta-analytic activation map is created for many (cognitive) terms, and these maps may be correlated to a given statistical map to identify terms with which they have the strongest relationship. This approach can identify indirect associations to cognitive terms used across a wide-range of previously published task-based functional neuroimaging studies, without relying on cognitive tasks acquired in the same cohort. Indeed, meta-analytic decoding has been used by several groups to evaluate the cognitive associations of their neuroimaging findings [*e.g.,* (Chang et al., 2013; Margulies et al., 2016; Paquola et al., 2019; Vogel et al., 2020; Vos de Wael et al., 2018)].

For each term in the term-based meta-analytical Neurosynth database, we computed which studies used the term with a frequency of at least 1 in 1000 words (default parameter in NiMARE). Next, the meta-analytic maps were computed for these labels using a multilevel kernel density Chi-square analysis implemented in NiMARE (Salo et al., 2020; Wager et al., 2007). For any user-provided surface-based statistical map, we interpolate the map from surface to volume space. Lastly, for every meta-analytic map in the database, we compute a voxel-wise product-moment correlation between the meta-analytic and statistical map. An example of retrieving correlations with meta-analytic terms for the *t*-statistic map computed earlier is shown in Fig. 3.

Fig. 3. Meta-analytic decoding. (A) Using the NiMARE toolbox (Salo et al., 2020) and the Neurosynth database (Yarkoni et al., 2011), we derived feature maps for every feature name in the Neurosynth database. We show an example association map for the terms "memory" and "reward". (B) Example Python code for computing the correlations between the *t*-statistic map and every term in the Neurosynth database, and plotting these correlations as a word cloud. This code as well as the MATLAB equivalent can be found in the supplemental Jupyter notebook and live script. (C) The resultant word cloud from the code in Fig. 3B.

A

```python
import seaborn as sns
import matplotlib.pyplot as plt
from brainstat.datasets import fetch_gradients

functional_gradients = fetch_gradients("fsaverage5", "margulies2016")

# Create kernel density plot.
df = pd.DataFrame({"x": slm.t.flatten(), "y": functional_gradients[:, 0]})
df.dropna(inplace=True)

_, ax = plt.subplots()
sns.kdeplot(x=df.x, y=df.y, fill=True, ax=ax, cmap="Blues")

ax.spines["right"].set_visible(False)
ax.spines["top"].set_visible(False)

plt.xlabel("t-statistic", fontdict={"fontsize": 20})
plt.ylabel("Functional Gradient 1", fontdict={"fontsize": 20})

plt.plot(np.unique(df.x), np.poly1d(np.polyfit(df.x, df.y, 1))(np.unique(df.x)), "k")
plt.text(-3.5, 6, f"ρ={df.x.corr(df.y, method='spearman'):.2f}", fontdict={"size": 20})
plt.gcf().subplots_adjust(left=0.2)

ax.set_xlim(-4.0, 4.0)
ax.set_ylim(-0.13, 0.15)
plt.xticks([-4.0, 4.0], fontsize=20)
plt.yticks([-12, 13], fontsize=20)
```

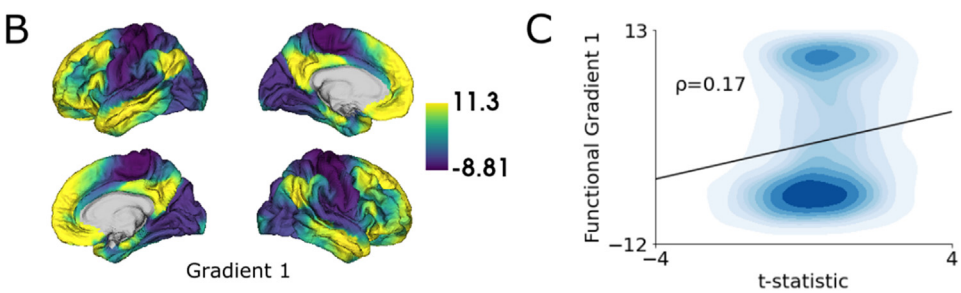

Fig. 4. Association to functional gradients. (A) Example Python code for computing and plotting the correlation of the t-statistic map and the first functional gradient. Cortical surface plotting code was omitted for brevity. See the supplemental Jupyter notebook (Python) and live script (MATLAB) for executable versions of this code as well as additional figure building code. (B) First functional gradient plotted onto the brain surface. (C) Kernel density plot of the t-statistic map and the first functional gradient.

3.2. Resting-state motifs

The functional architecture of the brain at rest has been described both as a set of continuous dimensions, called gradients (Margulies et al., 2016; Vos de Wael et al., 2020). These gradients highlight gradual transitions between regions and can be used to embed findings into the functional architecture of the human brain by assessing point-wise relationships with other markers. Prior studies have used functional gradients to assess the relationship of the brain's functional architecture to high level cognition (Murphy et al., 2019; Shine et al., 2019), hippocampal subfield connectivity (Vos de Wael et al., 2018), amyloid beta expression and aging (Lowe et al., 2019), microstructural organization (Huntenburg et al., 2017; Paquola et al., 2019), phylogenetic changes (Xu et al., 2020), and alterations in disease states (Caciagli et al., 2021; Hong et al., 2019; Tian et al., 2019).

The functional gradients included with BrainStat were derived from a resampled mean functional connectivity matrix of the S1200 release to fsaverage5 (to reduce computational complexity). Connectome gradients were subsequently computed. with BrainSpace using the following parameters: cosine similarity kernel, diffusion map embedding, *alpha=0.5, sparsity=0.9*, and *diffusion_time=0* (Vos de Wael et al., 2020). Example code for computing correlations between the first functional gradient and the *t*-statistic map are shown in Fig. 4. We find a low Spearman correlation (ρ=0.17) between these two maps. However, to test for significance of this correlation we need to correct for the spatial autocorrelation in the data (Markello and Misic, 2021). Three such corrections, namely spin test (Alexander-Bloch et al., 2018), Moran spectral randomization (Wagner and Dray, 2015), and variogram matching (Burt et al., 2020), are included in BrainSpace (Vos de Wael et al., 2020), a dependency of BrainStat.

3.3. Genetic expression

The Allen Human Brain Atlas (Hawrylycz et al., 2012) is a database of microarray gene expression data of over 20,000 genes derived from *post mortem* tissue samples obtained from six adult donors. This resource can be used to derive associations between neuroimaging data and molecular factors (Arnatkeviciute et al., 2021a) and, thus, yields insights into the mechanisms giving rise to anatomical and connectomic markers. For example, such data may be used to study associations between genetic factors and functional connectivity (Cioli et al., 2014; Krienen et al., 2016; Richiardi et al., 2015), anatomical connectivity (Goel et al., 2014; Park et al., 2021a), as well as alterations of connectivity in disease (Park et al., 2021b; Romme et al., 2017, Lariviere et al. 2022). The genetic decoding module of BrainStat leverages the abagen toolbox (Markello et al., 2021) to compute genetic expression data for a given parcellation. Default parameters from abagen follow guidelines established (Arnatkevičiūtė et al., 2019) and perform the following procedure. First, it fetches and updates the MNI152 coordinates of tissue samples of all six donors using coordinates provided by the *alleninf* package (https://github.com/chrisgorgo/alleninf). Next, it performs an intensity-based filtering of the probes to remove those

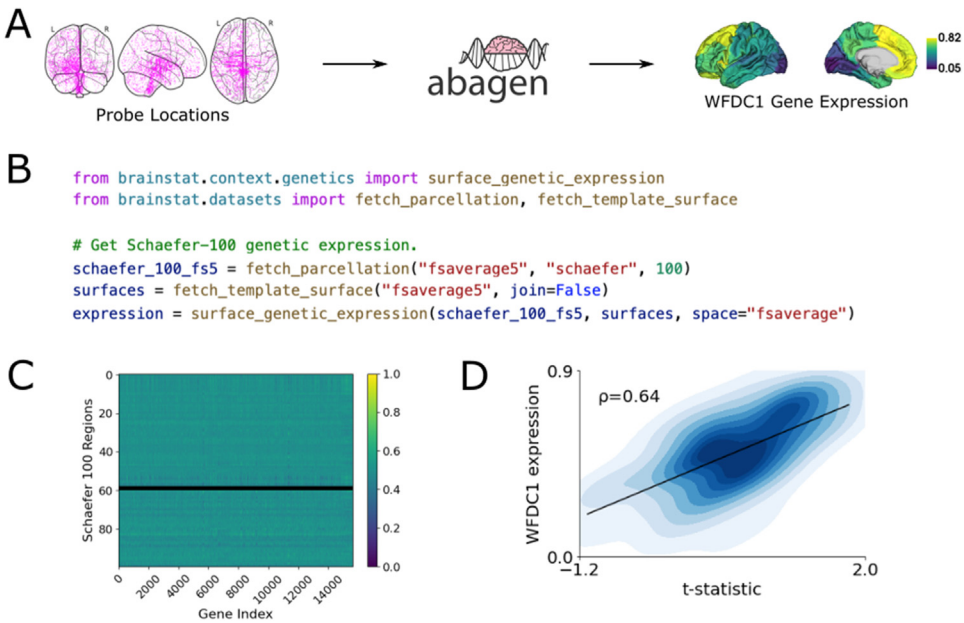

Fig. 5. Association to genetic expression. (A) BrainStat leverages data from the Allen Human Brain Atlas (Hawrylycz et al., 2012), provided by the Allen Institute for Brain Science, and processed with abagen (Markello et al., 2021) to derive transcription levels of thousands of genes. Shown are the locations of all probes as well as the expression of a single gene (WFDC1) within 100 functionally defined regions (Schaefer et al., 2017). (B) Example Python code for computing the genetic expression based on a surface parcellation. (C) The genetic expression matrix depicts the genetic expression, normalized to a range of [0, 1], of all parsed genes across all parcels. Black rows denote regions without samples. (D) Correlation between the *t*-statistic map and the WFDC1 gene expression. Figure plotting code was omitted for brevity. See the supplemental Jupyter notebook (Python) and live script (MATLAB) for executable versions of this code as well as additional figure building code.

that do not exceed background noise. Subsequently, for probes indexing the same gene, it selects the probe with the highest differential stability across donors. The tissue samples are then matched to regions in the parcellation scheme. Expression values for each sample across genes and for each gene across samples are normalized using a scaled robust sigmoid normalization function. Lastly, samples within each region are averaged within each donor, then averaged across donors. For details on the procedures with non-default parameters please consult the abagen documentation (https://abagen.readthedocs.io/). In Python, BrainStat calls abagen directly, and as such all parameters may be modified. In MATLAB, where abagen is not available, we included genetic expression matrices precomputed with abagen with default parameters for many common parcellation schemes. In Fig. 5, we show an example of fetching the genetic expression for a previously defined functional atlas (Schaefer et al., 2017), and correlating the output to the *t*-statistic map. The expression derived from this module can then be used in further analyses, for example by deriving the principal component of genetic expression and comparing it to previously derived statistical maps.

3.4. Histology

The BigBrain atlas (Amunts et al., 2013) is a three-dimensional reconstruction of a sliced and cell-body-stained human brain. With a digitized isotropic resolution of 20 micrometers, it is the first openly available whole-brain 3D histological dataset. As such, it is well suited for relating neuroimaging markers to histological properties. This resource can be used, for example, to cross-validate MRI-derived microstructural findings (Paquola et al., 2019; Royer et al., 2020), defining regions of interest based on histological properties (Sitek et al., 2019), or relating connectomic markers to microstructure (Arnatkeviciute et al., 2021b). The histology submodule aims to simplify the integration of neuroimaging findings with the BigBrain dataset. This submodule uses surfaces sampled from the BigBrain atlas (Amunts et al., 2013), at 50 different depths across the cortical mantle (Paquola et al., 2021). Covariance of these profiles, also known as microstructural profile covariance (Paquola et al., 2019), is computed with a partial correlation correcting for the mean intensity profile. Principal axes of cytoarchitectural variation are computed from microstructural profile covariance using BrainSpace with default parameters (Vos de Wael et al., 2020). An example of this is shown in Fig. 6. We find a correlation between the first eigenvector and the t-statistic map of ρ=-0.28.

Table 1
Run time evaluation. Time in seconds to solve a generic linear model for Python/Matlab code. The script involves defining the terms (*here,* Age, Sex), fitting the models (*here,* M= 1 + Age + Sex), building the contrast (*here,* -Age), as well as multiple comparison correction (via False Discovery Rate and Random Field Theory). Data are represented on fsaverage5 surfaces (20,484 vertices). Computations have been run on a MacBook Pro (2.9 GHZ quad core intel i7, 16 GB Memory, with Matlab R2022a and Python 3.9), and shown are average run times across 10 runs with the same model in seconds. Two times are presented for Matlab, with/without implicit parallelization. Surrogate datasets were generated using bootstrap-based resampling of included subjects.

	Model: Y=b0 + b1x1 + b2x	
Dataset	Python	Matlab
Tutorial data (n=82)	1.96±0.08	2.90±0.07/3.03±0.11
Surrogate data 1 (n=82)	2.08±0.03	2.87±0.04/3.10±0.16
Surrogate data 2 (n=700)	2.98±0.11	3.72±0.19/6.64±0.38
Surrogate data 3 (n=7000)	12.14±2.57	11.95±0.04/10.49±0.61

3.5. Run time evaluations

Despite being currently a single threaded implementation in both Matlab and Python, BrainStat heavily relies on matrix multiplications and allows for fast computations, even when larger datasets are analyzed. As an example, we performed a series of experiments on our test data and used bootstrap approaches to scale up simulated datasets to assess computation time (Table 1).

4. Discussion

The analysis of brain imaging data demands tools for uni- and multivariate statistical inference, and increasingly leverages data from multiple resources to facilitate interpretation and contextualization of significant results. Although many tools have been made available by the neuroimaging community to perform individual analytical steps (Larivière et al., 2021; Markello et al., 2022, 2021; Paquola et al., 2021; Salo et al., 2020; Yarkoni et al., 2011), there is currently no package that unifies statistical inference and contextualization approaches. Indeed, several previous tools allow for statistical analysis of neuroimaging data, including SPM in Matlab (https://www.fil.ion.ucl.ac.uk/spm/) SurfS-

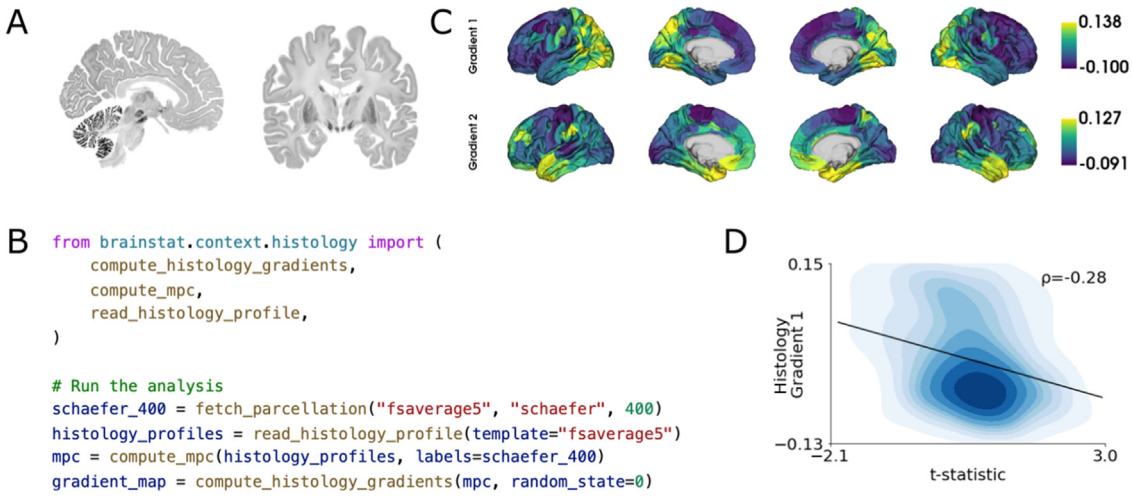

Fig. 6. Association to histological markers. (A) Selected sagittal and coronal slices from the BigBrain atlas. (B) Example Python code for computing gradients of microstructural profile covariance for the Schaefer-400 parcellation. Histology profiles, as computed in the BigBrainWarp toolbox, are loaded. From these profiles, a microstructural profile covariance matrix is built, and used to compute gradients of histology. (C) Gradients derived from the microstructural profile covariance of the BigBrain atlas. (D) The scatter plot of the *t*-statistic map and the first gradient of microstructural profile covariance. Figure plotting code was omitted for brevity. See the supplemental Jupyter notebook (Python) and live script (MATLAB) for executable versions of this code as well as additional figure building code.

tat in Matlab (https://www.math.mcgill.ca/keith/surfstat/), as well as nilearn in Python (https://nilearn.github.io/), among others. Furthermore, multiple resources allow for contextualization of findings, including neuromaps (https://github.com/netneurolab/neuromaps) and the ENIGMA toolbox (https://enigma-toolbox.readthedocs.io/). By being the only tool (*i*) that natively combines statistical analysis and contextualization, and (*ii*) that is implemented in both Python and Matlab, BrainStat aims to further facilitate and consolidate analytical workflows as a fully open access tool. We hope that this parallel implementation will facilitate teaching and training of analysts and researchers working in the field. Notably, the modular setup of the toolbox allows running statistical and contextualization analyses independent from one another. Furthermore, BrainStat is complemented with a thorough and easy-to-follow online documentation, providing novice and expert users alike an entry into integrated analyses of brain imaging data.

Linear models are a core technique for neuroimaging-based inference. Many common univariate and multivariate statistical analyses, including *t*-tests, F-tests, multiple linear regression, and (M)AN(C)OVA, can be considered special cases of the general linear model (Friston, 2005; Nichols and Holmes, 2002). As such, usage of general linear models is widespread throughout the neuroimaging literature [*e.g.*, (Bernhardt et al., 2018; Clarkson et al., 2011; Truong et al., 2013)]. Despite their prevalence, their implementation is not trivial. BrainStat's statistics module aims to provide a flexible multivariate linear modeling framework for neuroimaging data (Worsley et al., 2009). The focus of this manuscript was to present the possibilities provided by BrainStat, and outline an accessible tutorial for the toolbox's key functionality. As such, we illustrate the use of mixed effects models for testing the effects of age on cortical thickness. However, given the versatility of linear models, a large variety of models may be specified within the same framework. The flexible specification of a contrast simplifies testing of fitted models, with the toolbox furthermore providing initial quality control functions to verify model assumptions and model fit.

Recent years have seen an uptick in the usage of external datasets for the contextualization of MRI-derived results (Markello et al., 2022). These datasets can be leveraged for their unique advantages such as the unprecedented spatial resolution of the BigBrain histological atlas (Amunts et al., 2013), the vast number of task-fMRI studies included in the Neurosynth meta-analytical database (Yarkoni et al., 2011), and 3D maps of *post mortem* human brain gene expression information aggregated in the Allen Human Brain Atlas (Hawrylycz et al., 2012). These external datasets allow for more comprehensive studies of brain organization and may advance our understanding of fundamental principles of brain organization (Hansen et al., 2021; Larivière et al., 2019). Prior studies have used these datasets to relate task meta-analyses, genetic expression, and histology to markers of morphology (Valk et al., 2020; Wagstyl et al., 2020; Whitaker et al., 2016), function (Benkarim et al., 2021; Krienen et al., 2016; Margulies et al., 2016; Paquola et al., 2019), and structural connectivity (Romme et al., 2017; Vos de Wael et al., 2021). Though numerous packages exist to enable these analyses (Markello et al., 2021; Paquola et al., 2021; Salo et al., 2020; Yarkoni et al., 2011), these are generally distributed independently and their integration requires expertise, and often proficiency in specific programming languages as there are generally no cross-language implementations. BrainStat brings these tools together into a unified multi-language framework, thereby increasing their accessibility and streamlining the analytics processes of neuroimaging studies. It is of note that while the context module works natively with BrainStat-derived outputs, it is also possible to run this tool on other results (results obtained from other statistical packages, or simple brain feature maps). Collectively, the functionalities and datasets of the context module pave the way for enrichment analysis of research discoveries with respect to aspects of micro- and macroscale brain organization. Ultimately, we hope to reduce the barrier to entry of these techniques, reduce the chances of human error, and thereby accelerate cross-modal research in the neuroimaging community.

In its current implementation, BrainStat implements workflows for contextualization against microscale (*i.e.*, transcriptomic and histological) and functional (*e.g.*, fMRI meta-analyses and resting-state networks) features. This allows users to adopt increasingly popular analytical approaches in basic and clinical neuroimaging. It is worth noting that in general, the application of contextual association analysis does not necessarily imply any assumption on the directionality of associations between micro- and macroscale properties of brain organization, nor between structure and function. Indeed, microscale-macroscale associations (Arnatkeviciute et al., 2021; Fornito et al., 2019; Scholtens et al., 2022; Wang et al., 2022; Markello et al., 2021) as well as structure-function relationships (Benkarim et al., 2022; Goñi et al., 2014; Honey et al., 2009; Paquola et al., 2022; Suárez et al., 2020) in the human brain, remain a topic of highly active research, often suggesting complex, and bidirectional relations between different domains.

For task-based meta-analytical decoding, the current implementation of BrainStat interfaces with nimare (Salo et al. 2020), which performs meta-analytical inference in voxel (*i.e.*, MNI152) space. One potential limitation of this approach is that surface-to-voxel transformations do per se not lead to a dense representation within the cortical ribbon. BrainStat thus uses a ribbon-filling approach with either linear or nearest neighbor interpolation to generate a voxel-based approximation of a given surface map that is then cross-referenced in NiMARE. This step was chosen to avoid generating a surface-based clone of the (possibly evolving) NiMARE database. We would, furthermore, like to emphasize that future updates to BrainStat could capitalize on ongoing advances in meta-analytic decoding methods and tools to enhance reliability and interpretability. As an example, the use of topic-based meta-analysis using Latent Dirichlet allocation (LDA) to determine the meta-analytic sample of studies may provide a broader set of terms for each meta-analytic map, addressing drawbacks of term-based meta-analytic methods, notably redundancy and ambiguity of single terms. In particular, generalized Correspondence LDA (GC-LDA) has been suggested to add spatial and semantic constraints (Rubin et al. 2017), providing an even more nuanced functional decoding. Expanding from the Neurosynth database, the NeuroQuery database contains more extensive vocabulary and a richer representation of the studies' text, thereby adding nuance and precision in associating brain activations with written study content (Dockès et al. 2020).

Theoretical and empirical studies have shown the importance of replicability in science (Ioannidis, 2005; Moonesinghe et al., 2007; Open Science Collaboration, 2015). The proliferation of open-access datasets (Di Martino et al., 2014; Miller et al., 2016; Royer et al., 2021; Van Essen et al., 2013) and software (Fischl, 2012; Marcus et al., 2011; Paquola et al., 2021; Tournier et al., 2012; Vos de Wael et al., 2020) may increase reproducibility by allowing others to redo experiments with identical data and procedures, as well as reducing human error in the analysis (Milham et al., 2018; Poldrack et al., 2017). BrainStat may contribute to this process. By unifying statistical processing and multidomain feature association into a single package across two programming languages, the resulting code will require less customization and technical expertise from the end-user. Furthermore, BrainStat may increase the accessibility to all these methods for researchers in places that lack the institutional expertise to set up such integrated pipelines. Researchers and users are encouraged to contribute to continuously enhance functionality and scope of the BrainStat toolbox. Users seeking help are encouraged to post their questions to the GitHub Issues page (https://github.com/MICA-MNI/BrainStat/issues). Similarly, integration of new analytic methods from users around the world is supported through GitHub pull requests (https://github.com/MICA-MNI/BrainStat/pulls) and can be made part of future releases.

5. Methods

5.1. Tutorial dataset

We studied 70 healthy participants [30 females, age = 31.9 ± 8.9 (mean±SD); 12 of them (five female) came in for a second visit with age = 32.8 ± 7.5] of the MICS dataset (Royer et al., 2021). Note that these data include subjects not part of the current MICS release. The Ethics Committee of the Montreal Neurological Institute and Hospital approved the study, and written informed consent was obtained from all participants. For each visit, two T1w images were derived with the following parameters: MP-RAGE; 0.8mm isotropic voxels, matrix = 320×320, 224 sagittal slices, TR = 2300ms, TE = 3.14ms, TI = 900ms, flip angle = 9°, iPAT = 2, partial Fourier = 6/8. Scans were visually inspected for motion artefacts. Processing was performed with micapipe (https://github.com/MICA-MNI/micapipe). In short, cortical surface segmentations were generated from the T1w scans using Freesurfer 6.0 (Fischl, 2012). Participant's cortical thickness estimates were transformed to the fsaverage5 template and smoothed with a 10mm full-width-at-half-maximum Gaussian kernel.

Data and code availability

BrainStat is freely available through PyPi (https://pypi.org/project/brainstat/; installable with 'pip install brainstat'), FileExchange (https://www.mathworks.com/matlabcentral/fileexchange/89827-brainstat; installable with the add-on manager in MATLAB), and GitHub (https://github.com/MICA-MNI/BrainStat). Documentation is available at https://brainstat.readthedocs.io/. BrainStat supports Python 3.7-3.9 and MATLAB R2019b+ on Windows, macOS, and Linux. However, we advise users to consult the installation guide in our documentation for up-to-date requirements. All data used herein can be accessed through the BrainStat data loaders.

The examples provided in the paper are available on the Github repository (*Matlab*: https://github.com/MICA-MNI/BrainStat/blob/master/extra/nimg_figures_matlab_code.mlx; *Python*: https://github.com/MICA-MNI/BrainStat/blob/master/extra/nimg_figures_python_code.ipynb).

Moreover, our tutorials on linear models (*Matlab*: https://brainstat.readthedocs.io/en/master/matlab/tutorials/tutorial_1.html; *Python*: https://brainstat.readthedocs.io/en/master/python/generated_tutorials/plot_tutorial_01_basics.html) and context decoding (*Matlab*: https://brainstat.readthedocs.io/en/master/matlab/tutorials/tutorial_2.html; *Python*: https://brainstat.readthedocs.io/en/master/python/generated_tutorials/plot_tutorial_02_context.html) are also available on the GitHub repository.

Ethics statement

The data used here were retrieved from the MICA-MICs dataset (Royer et al., 2021). The Ethics Committee of the Montreal Neurological Institute and Hospital approved the MICA-MICs study (2018-3469). Written informed consent, including a statement for openly sharing all data in anonymized form, was obtained from all participants.

Author contributions

R.V., Ş.B., and S.L. were the lead developers of the toolbox. O.B., P.H., S.V, and B.B. further assisted in toolbox design. R.V., S.L., and B.B. drafted the manuscript. All authors assisted in revising the manuscript.

Funding

S.L. acknowledges funding from the Canadian Institutes of Health Research (CIHR) and the Richard and Ann Sievers award. O.B. was funded by a Healthy Brains, Healthy Lives (HBHL) postdoctoral fellowship and the Quebec Autism Research Training (QART) program. R.V.d.W. was funded by the Richard and Ann Sievers award. P.H. was supported in parts by funding from the Canada First Research Excellence Fund, awarded to McGill University for the HBHL initiative, the National Institutes of Health (NIH) NIH-NIBIB P41 EB019936 (ReproNim), the National Institute Of Mental Health of the NIH under Award Number R01MH096906, a research scholar award from Brain Canada, in partnership with Health Canada, for the Canadian Open Neuroscience Platform initiative, as well as an Excellence Scholarship from Unifying Neuroscience and Artificial Intelligence - Québec. R.R.C. received support from the Fonds de la Recherche du Québec – Santé (FRQ-S). C.P. was funded by Helmholtz International BigBrain Analytics Learning Laboratory (HIBALL). S.J.H. was funded by was supported by funding from the Brain & Behavior Research Foundation (NARSAD Young Investigator grant; #28436) and the Institute for Basic Science (IBS-R15-D1) in Korea. B.M. acknowledges support from the Natural Sciences and Engineering Research Council of Canada (NSERC), CIHR, the Canada Research Chairs Program (CRC), Brain Canada Future Leaders, and HBHL. S.L.V.

acknowledges support from the Otto Hahn award from the Max Planck society and HIBALL. B.B. acknowledges research support from the National Science and Engineering Research Council of Canada (NSERC Discovery-1304413), CIHR (FDN-154298, PJT174995), SickKids Foundation (NI17-039), Azrieli Center for Autism Research (ACAR), BrainCanada, FRQ-S, HBHL, and CRC. A.E. and B.B. furhtermore acknowledge funding from HIBALL.

Declaration of Competing Interest

The authors declare that they have no known competing financial interests or personal relationships that could have appeared to influence the work reported in this paper.

Credit authorship contribution statement

Sara Larivière: Conceptualization, Methodology, Software, Writing – original draft. **Şeyma Bayrak:** Conceptualization, Methodology, Software, Writing – original draft. **Reinder Vos de Wael:** Conceptualization, Methodology, Software, Writing – original draft. **Oualid Benkarim:** Software, Writing – review & editing. **Peer Herholz:** Software, Writing – review & editing. **Raul Rodriguez-Cruces:** Software, Writing – review & editing. **Casey Paquola:** Writing – review & editing. **Seok-Jun Hong:** Writing – review & editing. **Bratislav Misic:** Writing – review & editing. **Alan C. Evans:** Writing – review & editing. **Sofie L. Valk:** Conceptualization, Methodology, Software, Writing – original draft, Supervision. **Boris C. Bernhardt:** Conceptualization, Methodology, Software, Writing – original draft, Supervision.

Acknowledgments

The authors would like to thank the late Keith Worsley for his invaluable work on the SurfStat toolbox, which inspired BrainStat.

Supplementary materials

Supplementary material associated with this article can be found, in the online version, at doi:10.1016/j.neuroimage.2022.119807.

References

Alexander-Bloch, A.F., Shou, H., Liu, S., Satterthwaite, T.D., Glahn, D.C., Shinohara, R.T., Vandekar, S.N., Raznahan, A., 2018. On testing for spatial correspondence between maps of human brain structure and function. Neuroimage doi:10.1016/j.neuroimage.2018.05.070.

Amunts, K., Lepage, C., Borgeat, L., Mohlberg, H., Dickscheid, T., Rousseau, M.-É., Bludau, S., Bazin, P.-L., Lewis, L.B., Oros-Peusquens, A.-M., 2013. BigBrain: an ultrahigh-resolution 3D human brain model. Science 340, 1472–1475.

Arnatkeviciute, A., Fulcher, B.D., Bellgrove, M.A., Fornito, A., 2021a. Imaging transcriptomics of brain disorders. Biol. Psychiatry Glob. Open Sci. doi:10.1016/j.bpsgos.2021.10.002.

Arnatkeviciute, A., Fulcher, B.D., Oldham, S., Tiego, J., Paquola, C., Gerring, Z., Aquino, K., Hawi, Z., Johnson, B., Ball, G., Klein, M., Deco, G., Franke, B., Bellgrove, M.A., Fornito, A., 2021b. Genetic influences on hub connectivity of the human connectome. Nat. Commun. 12, 4237. doi:10.1038/s41467-021-24306-2.

Arnatkeviciute, A., Fulcher, B.D., Fornito, A., 2019. A practical guide to linking brain-wide gene expression and neuroimaging data. Neuroimage 189, 353–367. doi:10.1016/j.neuroimage.2019.01.011.

Arnatkeviciute, A., Fulcher, B.D., Bellgrove, M.A., Fornito, A., 2021. Where the genome meets the connectome: understanding how genes shape human brain connectivity. Neuroimage 244, 118570. doi:10.1016/j.neuroimage.2021.118570.

Benjamini, Y., Hochberg, Y., 1995. Controlling the false discovery rate: a practical and powerful approach to multiple testing. J. R. Stat. Soc. 57 (1), 289–300.

Benkarim, O., Paquola, C., Park, B., Hong, S.-J., Royer, J., Vos de Wael, R., Lariviere, S., Valk, S., Bzdok, D., Mottron, L., 2021. Connectivity alterations in autism reflect functional idiosyncrasy. Commun. Biol. 4, 1–15.

Benkarim, O., Paquola, C., Park, B.Y., Royer, J., Rodríguez-Cruces, R., de Wael, R.V., Misic, B., Piella, G., Bernhardt, B.C., 2022. A Riemannian approach to predicting brain function from the structural connectome. Neuroimage, 119299.

Bernhardt, B.C., Fadaie, F., Vos de Wael, R., Hong, S.J., Liu, M., Guiot, M.C., Rudko, D.A., Bernasconi, A., Bernasconi, N., 2018. Preferential susceptibility of limbic cortices to microstructural damage in temporal lobe epilepsy: a quantitative T1 mapping study. Neuroimage 182, 294–303. doi:10.1016/j.neuroimage.2017.06.002.

Burt, J.B., Helmer, M., Shinn, M., Anticevic, A., Murray, J.D., 2020. Generative modeling of brain maps with spatial autocorrelation. Neuroimage 220, 117038. doi:10.1016/j.neuroimage.2020.117038.

Caciagli, L., Paquola, C., He, X., Vollmar, C., Centeno, M., Wandschneider, B., Braun, U., Trimmel, K., Vos, S.B., Sidhu, M.K., others, 2021. Disorganization of language and working memory systems in frontal versus temporal lobe epilepsy. medRxiv.

Cameron, C., Sharad, S., Brian, C., Ranjeet, K., Satrajit, G., Chaogan, Y., Qingyang, L., Daniel, L., Joshua, V., Randal, B., Stanley, C., Maarten, M., Clare, K., Adriana, D.M., Francisco, C., Michael, M., 2013. Towards automated analysis of connectomes: the configurable pipeline for the analysis of connectomes (C-PAC). Front. Neuroinform 7. doi:10.3389/conf.fninf.2013.09.00042.

Casey, B.J., Cannonier, T., Conley, M.I., Cohen, A.O., Barch, D.M., Heitzeg, M.M., Soules, M.E., Teslovich, T., Dellarco, D.V., Garavan, H., Orr, C.A., Wager, T.D., Banich, M.T., Speer, N.K., Sutherland, M.T., Riedel, M.C., Dick, A.S., Bjork, J.M., Thomas, K.M., Chaarani, B., Mejia, M.H., Hagler, D.J., Daniela Cornejo, M., Sicat, C.S., Harms, M.P., Dosenbach, N.U.F., Rosenberg, M., Earl, E., Bartsch, H., Watts, R., Polimeni, J.R., Kuperman, J.M., Fair, D.A., Dale, A.M., 2018. The Adolescent Brain Cognitive Development (ABCD) study: imaging acquisition across 21 sites. Developmental Cognitive Neuroscience. Adolesc. Brain Cogn. Dev. (ABCD) Consortium: Rationale, Aims, and Assessment Strategy 32, 43–54. doi:10.1016/j.dcn.2018.03.001.

Chang, L.J., Yarkoni, T., Khaw, M.W., Sanfey, A.G., 2013. Decoding the role of the insula in human cognition: functional parcellation and large-scale reverse inference. Cereb. Cortex 23, 739–749. doi:10.1093/cercor/bhs065.

Cioli, C., Abdi, H., Beaton, D., Burnod, Y., Mesmoudi, S., 2014. Differences in human cortical gene expression match the temporal properties of large-scale functional networks. PLoS One 9, e115913. doi:10.1371/journal.pone.0115913.

Clarkson, M.J., Cardoso, M.J., Ridgway, G.R., Modat, M., Leung, K.K., Rohrer, J.D., Fox, N.C., Ourselin, S., 2011. A comparison of voxel and surface based cortical thickness estimation methods. NeuroImage, Special Issue: Educational Neuroscience 57, 856–865. doi:10.1016/j.neuroimage.2011.05.053.

Collins, D.L., Zijdenbos, A.P., Paus, T., Evans, A.C., 2003. Use of registration for cohort studies. Med. Image Registration.

Dadar, M., Fonov, V.S., Collins, D.L., Initiative, A.D.N., 2018. A comparison of publicly available linear MRI stereotaxic registration techniques. Neuroimage 174, 191–200.

Desikan, R.S., Ségonne, F., Fischl, B., Quinn, B.T., Dickerson, B.C., Blacker, D., Buckner, R.L., Dale, A.M., Maguire, R.P., Hyman, B.T., 2006. An automated labeling system for subdividing the human cerebral cortex on MRI scans into gyral based regions of interest. Neuroimage 31, 968–980.

Di Martino, A., Yan, C.-G., Li, Q., Denio, E., Castellanos, F.X., Alaerts, K., Anderson, J.S., Assaf, M., Bookheimer, S.Y., Dapretto, M., Deen, B., Delmonte, S., Dinstein, I., Ertl-Wagner, B., Fair, D.A., Gallagher, L., Kennedy, D.P., Keown, C.L., Keysers, C., Lainhart, J.E., Lord, C., Luna, B., Menon, V., Minshew, N.J., Monk, C.S., Mueller, S., Müller, R.-A., Nebel, M.B., Nigg, J.T., O'Hearn, K., Pelphrey, K.A., Peltier, S.J., Rudie, J.D., Sunaert, S., Thioux, M., Tyszka, J.M., Uddin, L.Q., Verhoeven, J.S., Wenderoth, N., Wiggins, J.L., Mostofsky, S.H., Milham, M.P., 2014. The autism brain imaging data exchange: towards a large-scale evaluation of the intrinsic brain architecture in autism. Mol. Psychiatry 19, 659–667. doi:10.1038/mp.2013.78.

Dokès, J, Podrack, RA, Primet, R, Gözükan, H, Yarkoni, T, Suchanek, F, Thirion, B, Varoquaux, G, 2020. Neuroquery, comprehensive meta-analysis of human brain mapping. Elife 9, e53385.

Eklund, A., Nichols, T.E., Knutsson, H., 2016. Cluster failure: why fMRI inferences for spatial extent have inflated false-positive rates. Proc. Natl Acad. Sci. 113, 7900–7905. doi:10.1073/pnas.1602413113.

Esteban, O., Markiewicz, C.J., Blair, R.W., Moodie, C.A., Isik, A.I., Erramuzpe, A., Kent, J.D., Goncalves, M., DuPre, E., Snyder, M., Oya, H., Ghosh, S.S., Wright, J., Durnez, J., Poldrack, R.A., Gorgolewski, K.J., 2019. fMRIPrep: a robust preprocessing pipeline for functional MRI. Nat. Methods 16, 111–116. doi:10.1038/s41592-018-0235-4.

Fischl, B., 2012. FreeSurfer. Neuroimage 62, 774–781. doi:10.1016/j.neuroimage.2012.01.021.

Friston, K.J., 2005. Models of brain function in neuroimaging. Annu. Rev. Psychol. 56, 57–87. doi:10.1146/annurev.psych.56.091103.070311.

Fornito, A., Arnatkevičiūtė, A., Fulcher, B.D., 2019. Bridging the gap between connectome and transcriptome. Trends Cogn. Sci. 23 (1), 34–50. doi:10.1016/j.tics.2018.10.005.

Glasser, M.F., Coalson, T.S., Robinson, E.C., Hacker, C.D., Harwell, J., Yacoub, E., Ugurbil, K., Andersson, J., Beckmann, C.F., Jenkinson, M., 2016. A multi-modal parcellation of human cerebral cortex. Nature 536, 171. doi:10.1038/nature18933.

Glasser, M.F., Sotiropoulos, S.N., Wilson, J.A., Coalson, T.S., Fischl, B., Andersson, J.L., Xu, J., Jbabdi, S., Webster, M., Polimeni, J.R., Van Essen, D.C., Jenkinson, M., 2013. The minimal preprocessing pipelines for the Human Connectome Project. Neuroimage 80, 105–124. doi:10.1016/j.neuroimage.2013.04.127.

Goel, P., Kuceyeski, A., LoCastro, E., Raj, A., 2014. Spatial patterns of genome-wide expression profiles reflect anatomic and fiber connectivity architecture of healthy human brain. Hum. Brain Mapp. 35, 4204–4218.

Goñi, J., Van Den Heuvel, M.P., Avena-Koenigsberger, A., Velez de Mendizabal, N., Betzel, R.F., Griffa, A., Hagmann, P., Corominas-Murtra, B., Thiran, J.P., Sporns, O., 2014. Resting-brain functional connectivity predicted by analytic measures of network communication. Proc. Natl. Acad. Sci. 111 (2), 833–838.

Gordon, E.M., Laumann, T.O., Adeyemo, B., Huckins, J.F., Kelley, W.M., Petersen, S.E., 2016. Generation and evaluation of a cortical area parcellation from resting-state correlations. Cereb. Cortex 26, 288–303.

Hansen, J.Y., Markello, R.D., Vogel, J.W., Seidlitz, J., Bzdok, D., Misic, B., 2021. Mapping gene transcription and neurocognition across human neocortex. Nat. Hum. Behav. 5, 1240–1250. doi:10.1038/s41562-021-01082-z.

Hawrylycz, M.J., Lein, E.S., Guillozet-Bongaarts, A.L., Shen, E.H., Ng, L., Miller, J.A., van de Lagemaat, L.N., Smith, K.A., Ebbert, A., Riley, Z.L., Abajian, C., Beckmann, C.F.,

Bernard, A., Bertagnolli, D., Boe, A.F., Cartagena, P.M., Chakravarty, M.M., Chapin, M., Chong, J., Dalley, R.A., Daly, B.D., Dang, C., Datta, S., Dee, N., Dolbeare, T.A., Faber, V., Feng, D., Fowler, D.R., Goldy, J., Gregor, B.W., Haradon, Z., Haynor, D.R., Hohmann, J.G., Horvath, S., Howard, R.E., Jeromin, A., Jochim, J.M., Kinnunen, M., Lau, C., Lazarz, E.T., Lee, C., Lemon, T.A., Li, L., Li, Y., Morris, J.A., Overly, C.C., Parker, P.D., Parry, S.E., Reding, M., Royall, J.J., Schulkin, J., Sequeira, P.A., Slaughterbeck, C.R., Smith, S.C., Sodt, A.J., Sunkin, S.M., Swanson, B.E., Vawter, M.P., Williams, D., Wohnoutka, P., Zielke, H.R., Geschwind, D.H., Hof, P.R., Smith, S.M., Koch, C., Grant, S.G.N., Jones, A.R., 2012. An anatomically comprehensive atlas of the adult human brain transcriptome. Nature 489, 391–399. doi:10.1038/nature11405.

Honey, C.J., Sporns, O., Cammoun, L., Gigandet, X., Thiran, J.P., Meuli, R., Hagmann, P., 2009. Predicting human resting-state functional connectivity from structural connectivity. Proc. Natl. Acad. Sci. 106 (6), 2035–2040.

Hong, S.-J., Vos de Wael, R., Bethlehem, R.A.I., Lariviere, S., Paquola, C., Valk, S.L., Milham, M.P., Di Martino, A., Margulies, D.S., Smallwood, J., Bernhardt, B.C., 2019. Atypical functional connectome hierarchy in autism. Nat. Commun. 10, 1022. doi:10.1038/s41467-019-08944-1.

Huntenburg, J.M., Bazin, P.L., Goulas, A., Tardif, C.L., Villringer, A., Margulies, D.S., 2017. A Systematic Relationship Between Functional Connectivity and Intracortical Myelin in the. Hum. Cereb. Cortex. Cerebral cortex (New York, N.Y. : 1991) 27, 981–997. doi:10.1093/cercor/bhx030.

Ioannidis, J.P., 2005. Why most published research findings are false. PLoS Med. 2, e124.

Kim, J., Singh, V., Lee, JK, Lerch, J., Ad-Dab'bagh, Y., MacDonald, D., Lee, JM, Kim, S., Evans, A., 2005. Automated 3-D extraction and evaluation of the inner and outer cortical surfaces using a Laplacian map and partial volume effect classification. Neuroimage 27, 210–221.

Krienen, F.M., Yeo, B.T.T., Ge, T., Buckner, R.L., Sherwood, C.C., 2016. Transcriptional profiles of supragranular-enriched genes associate with corticocortical network architecture in the human brain. Proc. Natl. Acad. Sci. 113, E469–E478. doi:10.1073/pnas.1510903113.

Laird, A.R., Lancaster, J.J., Fox, P.T., 2005. Brainmap. Neuroinformatics 3, 65–77.

Larivière, S., Royer, J., Rodriguez-Cruces, R., Paquola, C., Caligiuri, M.E., Gambardella, A., Concha, L., Keller, S.S., 2022. Structural network alteratoions in focal and generalized epilepsy assessed in a worldwide ENIGMA study follow axes of epilepsy risk gene expression. Nat. Commun. 13 (1), 4320. doi:10.1038/s41467-022-31730-5.

Larivière, S., Paquola, C., Park, B., Royer, J., Wang, Y., Benkarim, O., Vos de Wael, R., Valk, S.L., Thomopoulos, S.I., Kirschner, M., 2021. The ENIGMA Toolbox: multiscale neural contextualization of multisite neuroimaging datasets. Nat. Methods 18, 698–700.

Larivière, S., Vos de Wael, R., Paquola, C., Hong, S.-J., Mišić, B., Bernasconi, N., Bernasconi, A., Bonilha, L., Bernhardt, B.C., 2019. Microstructure-informed connectomics: enriching large-scale descriptions of healthy and diseased brains. Brain Connect 9, 113–127. doi:10.1089/brain.2018.0587.

Lowe, A.J., Paquola, C., Vos de Wael, R., Girn, M., Lariviere, S., Tavakol, S., Caldairou, B., Royer, J., Schrader, V.D., Bernasconi, A., Bernasconi, N., Spreng, R.N., Bernhardt, B.C., 2019. Targeting age-related differences in brain and cognition with multimodal imaging and connectome topography profiling. Hum. Brain Mapp. 40, 5213–5230. doi:10.1002/hbm.24767.

Lyttelton, O., Boucher, M., Robbins, S., Evans, A., 2007. An unbiased iterative group registration template for cortical surface analysis. Neuroimage 34, 1535–1544.

Marcus, D., Harwell, J., Olsen, T., Hodge, M., Glasser, M., Prior, F., Jenkinson, M., Laumann, T., Curtiss, S., Van Essen, D., 2011. Informatics and data mining tools and strategies for the human connectome project. Front. Neuroinform. 5, 4.

Margulies, D.S., Ghosh, S.S., Goulas, A., Falkiewicz, M., Huntenburg, J.M., Langs, G., Bezgin, G., Eickhoff, S.B., Castellanos, F.X., Petrides, M., Jefferies, E., Smallwood, J., 2016. Situating the default-mode network along a principal gradient of macroscale cortical organization. Proc. Natl. Acad. Sci. U. S. A. 113, 12574–12579. doi:10.1073/pnas.1608282113.

Markello, R.D., Arnatkeviciute, A., Poline, J.-B., Fulcher, B.D., Fornito, A., Misic, B., 2021. Standardizing workflows in imaging transcriptomics with the abagen toolbox. Elife 10, e72129. doi:10.7554/eLife.72129.

Markello, R.D., Hansen, J.Y., Liu, Z.-Q., Bazinet, V., Shafiei, G., Suarez, L.E., Blostein, N., Seidlitz, J., Baillet, S., Satterthwaite, T.D., Chakravarty, M., Raznahan, A., Misic, B., 2022. Neuromaps: structural and functional interpretation of brain maps. https://doi.org/10.1101/2022.01.06.475081

Markello, R.D., Misic, B., 2021. Comparing spatial null models for brain maps. Neuroimage 236, 118052.

Milham, M.P., Craddock, R.C., Son, J.J., Fleischmann, M., Clucas, J., Xu, H., Koo, B., Krishnakumar, A., Biswal, B.B., Castellanos, F.X., Colcombe, S., Di Martino, A., Zuo, X.-N., Klein, A., 2018. Assessment of the impact of shared brain imaging data on the scientific literature. Nat. Commun. 9, 2818. doi:10.1038/s41467-018-04976-1.

Miller, K.L., Alfaro-Almagro, F., Bangerter, N.K., Thomas, D.L., Yacoub, E., Xu, J., Bartsch, A.J., Jbabdi, S., Sotiropoulos, S.N., Andersson, J.L., Griffanti, L., Douaud, G., Okell, T.W., Weale, P., Dragonu, I., Garratt, S., Hudson, S., Collins, R., Jenkinson, M., Matthews, P.M., Smith, S.M., 2016. Multimodal population brain imaging in the UK Biobank prospective epidemiological study. Nat. Neurosci. 19, 1523–1536. doi:10.1038/nn.4393.

Moonesinghe, R., Khoury, M.J., Janssens, A.C.J.W., 2007. Most published research findings are false—but a little replication goes a long way. PLoS Med. 4, e28. doi:10.1371/journal.pmed.0040028.

Murphy, C., Wang, H.-T., Konu, D., Lowndes, R., Margulies, D.S., Jefferies, E., Smallwood, J., 2019. Modes of operation: a topographic neural gradient supporting stimulus dependent and independent cognition. Neuroimage 186, 487–496.

Nichols, T.E., Holmes, A.P., 2002. Nonparametric permutation tests for functional neuroimaging: a primer with examples. Hum. Brain Mapp. 15, 1–25.

Open Science Collaboration, 2015. Estimating the reproducibility of psychological science. Science 349.

Paquola, C., Royer, J., Lewis, L.B., Lepage, C., Glatard, T., Wagstyl, K., DeKraker, J., Toussaint, P.-J., Valk, S.L., Collins, L., Khan, A.R., Amunts, K., Evans, A.C., Dickscheid, T., Bernhardt, B., 2021. BigBrainWarp: toolbox for integration of BigBrain 3D histology with multimodal neuroimaging. bioRxiv doi:10.1101/2021.05.04.442563, 2021.05.04.442563.

Paquola, C., Vos De Wael, R., Wagstyl, K., Bethlehem, R.A.I., Hong, S.-J., Seidlitz, J., Bullmore, E.T., Evans, A.C., Misic, B., Margulies, D.S., Smallwood, J., Bernhardt, B.C., 2019. Microstructural and functional gradients are increasingly dissociated in transmodal cortices. PLoS Biol. 17, e3000284. doi:10.1371/journal.pbio.3000284.

Paquola, C., Amunts, K., Evans, A., Smallwood, J., Bernhardt, B., 2022. Closing the mechanistic gap: the value of microarchitecture in understanding cognitive networks. Trends Cogn. Sci..

Park, B., Bethlehem, R.A., Paquola, C., Larivière, S., Rodríguez-Cruces, R., Vos de Wael, R., Bullmore, E.T., Bernhardt, B.C.Neuroscience in Psychiatry Network (NSPN) Consortium, 2021a. An expanding manifold in transmodal regions characterizes adolescent reconfiguration of structural connectome organization. Elife 10, e64694. doi:10.7554/eLife.64694.

Park, B., Hong, S.-J., Valk, S.L., Paquola, C., Benkarim, O., Bethlehem, R.A., Di Martino, A., Milham, M.P., Gozzi, A., Yeo, B.T., 2021b. Differences in subcortico-cortical interactions identified from connectome and microcircuit models in autism. Nat. Commun. 12, 1–15.

Poldrack, R.A., Baker, C.I., Durnez, J., Gorgolewski, K.J., Matthews, P.M., Munafò, M.R., Nichols, T.E., Poline, J.-B., Vul, E., Yarkoni, T., 2017. Scanning the horizon: towards transparent and reproducible neuroimaging research. Nat. Rev. Neurosci. 18, 115–126. doi:10.1038/nrn.2016.167.

Richiardi, J., Altmann, A., Milazzo, A.-C., Chang, C., Chakravarty, M.M., Banaschewski, T., Barker, G.J., Bokde, A.L.W., Bromberg, U., Büchel, C., Conrod, P., Fauth-Bühler, M., Flor, H., Frouin, V., Gallinat, J., Garavan, H., Gowland, P., Heinz, A., Lemaître, H., Mann, K.F., Martinot, J.-L., Nees, F., Paus, T., Pausova, Z., Rietschel, M., Robbins, T.W., Smolka, M.N., Spanagel, R., Ströhle, A., Schumann, G., Hawrylycz, M., Poline, J.-B., Greicius, M.D.IMAGEN CONSORTIUM, 2015. Correlated gene expression supports synchronous activity in brain networks. Science 348, 1241–1244. doi:10.1126/science.1255905.

Romme, I.A.C., de Reus, M.A., Ophoff, R.A., Kahn, R.S., van den Heuvel, M.P., 2017. Connectome Disconnectivity and Cortical Gene Expression in Patients With Schizophrenia. Biological Psychiatry. Schizophrenia 81, 495–502. doi:10.1016/j.biopsych.2016.07.012.

Royer, J., Paquola, C., Larivière, S., Vos de Wael, R., Tavakol, S., Lowe, A.J., Benkarim, O., Evans, A.C., Bzdok, D., Smallwood, J., Frauscher, B., Bernhardt, B.C., 2020. Myeloarchitecture gradients in the human insula: Histological underpinnings and association to intrinsic functional connectivity. Neuroimage 216, 116859. doi:10.1016/j.neuroimage.2020.116859.

Royer, J., Rodríguez-Cruces, R., Tavakol, S., Larivière, S., Herholz, P., Li, Q., Wael, R.V.de, Paquola, C., Benkarim, O., Park, B., Lowe, A.J., Margulies, D., Smallwood, J., Bernasconi, A., Bernasconi, N., Frauscher, B., Bernhardt, B.C., 2021. An Open MRI Dataset for Multiscale Neuroscience. bioRxiv doi:10.1101/2021.08.04.454795.

Rubin, TN, Koyejo, O, Gorgolewski, KJ, Jones, MN, Poldrack, RA, Yarkoni, T, 2017. Decoding brain activity using a large-scale probabilistic functional-anatomical atlas of human cognition. PLoS Comput. Biol. 13 (10), e1005649.

Salo, T., Yarkoni, T., Nichols, T.E., Poline, J.-B., Kent, J.D., Gorgolewski, K.J., Glerean, E., Bottenhorn, K.L., Bilgel, M., Wright, J., Reeders, P., Kimbler, A., Nielson, D.N., Yanes, J.A., Pérez, A., Oudyk, K.M., Jarecka, D., Laird, A.R., 2020. neurostuff/NiMARE: 0.0.5. Zenodo. https://doi.org/10.5281/zenodo.4408504

Salo, T., Bottenhorn, K.L., Nichols, T.E., Riedel, M.C., Sutherland, M.T., Yarkoni, T., Laird, A.R., 2018. NiMARE: a neuroimaging meta-analysis research environment. F1000Res 7.

Schaefer, A., Kong, R., Gordon, E.M., Laumann, T.O., Zuo, X.-N., Holmes, A.J., Eickhoff, S.B., Yeo, B.T., 2017. Local-global parcellation of the human cerebral cortex from intrinsic functional connectivity MRI. Cereb. Cortex 28, 3095–3114. doi:10.1093/cercor/bhx179.

Scholtens, L.H., Pijnenburg, R., de Lange, S.C., Huitinga, I., Van den Heuvel, M.P.Netherlands Brain Bank, 2022. Common microscale and macroscale principles of connectivity in the human brain. J. Neurosci. 42 (20), 4147–4163. doi:10.1523/JNEUROSCI.1572-21.2022.

Shine, J.M., Breakspear, M., Bell, P., Ehgoetz, M.K., Shine, R., Koyejo, O., Sporns, O., Poldrack, R., 2019. Human cognition involves the dynamic integration of neural activity and neuromodulatory systems. Nat. Neurosci. 22, 289–296.

Sitek, K.R., Gulban, O.F., Calabrese, E., Johnson, G.A., Lage-Castellanos, A., Moerel, M., Ghosh, S.S., De Martino, F., 2019. Mapping the human subcortical auditory system using histology, postmortem MRI and in vivo MRI at 7T. Elife 8, e48932. doi:10.7554/eLife.48932.

Suárez, L.E., Markello, R.D., Betzel, R.F., Misic, B., 2020. Linking structure and function in macroscale brain networks. Trends Cogn. Sci. 24 (4), 302–315.

Tian, Y., Zalesky, A., Bousman, C., Everall, I., Pantelis, C., 2019. Insula functional connectivity in schizophrenia: subregions, gradients, and symptoms. Biol. Psychiatry 4, 399–408.

Tournier, J.D., Calamante, F., Connelly, A., 2012. MRtrix: diffusion tractography in crossing fiber regions. Int. J. Imaging Syst. Technol. 22, 53–66. doi:10.1002/ima.22005.

Truong, W., Minuzzi, L., Soares, C.N., Frey, B.N., Evans, A.C., MacQueen, G.M., Hall, G.B.C., 2013. Changes in cortical thickness across the lifespan in major depressive disorder. Psychiatry Res. Neuroimaging 214, 204–211. doi:10.1016/j.pscychresns.2013.09.003.

Valk, S.L., Xu, T., Margulies, D.S., Masouleh, S.K., Paquola, C., Goulas, A., Kochunov, P., Smallwood, J., Yeo, B.T.T., Bernhardt, B.C., Eickhoff, S.B., 2020. Shaping brain struc-

ture: genetic and phylogenetic axes of macro scale organization of cortical thickness (preprint). Neuroscience doi:10.1101/2020.02.10.939561.

Van Essen, D.C., Smith, S.M., Barch, D.M., Behrens, T.E.J., Yacoub, E., Ugurbil, K., Consortium, W.U.-M.H.C.P., 2013. The WU-Minn human connectome project: an overview. Neuroimage 80, 62–79. doi:10.1016/j.neuroimage.2013.05.041.

Vogel, J.W., La Joie, R., Grothe, M.J., Diaz-Papkovich, A., Doyle, A., Vachon-Presseau, E., Lepage, C., Vos de Wael, R., Thomas, R.A., Iturria-Medina, Y., Bernhardt, B., Rabinovici, G.D., Evans, A.C., 2020. A molecular gradient along the longitudinal axis of the human hippocampus informs large-scale behavioral systems. Nat. Commun. 11, 960. doi:10.1038/s41467-020-14518-3.

Vos de Wael, R., Benkarim, O., Paquola, C., Lariviere, S., Royer, J., Tavakol, S., Xu, T., Hong, S.-J., Langs, G., Valk, S., 2020. BrainSpace: a toolbox for the analysis of macroscale gradients in neuroimaging and connectomics datasets. Commun. Biol. 3, 1–10.

Vos de Wael, R., Larivière, S., Caldairou, B., Hong, S.-J., Margulies, D.S., Jefferies, E., Bernasconi, A., Smallwood, J., Bernasconi, N., Bernhardt, B.C., 2018. Anatomical and microstructural determinants of hippocampal subfield functional connectome embedding. Proc. Natl. Acad. Sci. 115, 10154–10159.

Vos de Wael, R., Royer, J., Tavakol, S., Wang, Y., Paquola, C., Benkarim, O., Eichert, N., Larivière, S., Xu, T., Misic, B., Smallwood, J., Valk, S.L., Bernhardt, B.C., 2021. Structural Connectivity gradients of the temporal lobe serve as multiscale axes of brain organization and cortical evolution. Cereb. Cortex 31, 5151–5164. doi:10.1093/cercor/bhab149.

Wager, T.D., Lindquist, M., Kaplan, L., 2007. Meta-analysis of functional neuroimaging data: current and future directions. Soc. Cogn. Affect. Neurosci. 2, 150–158. doi:10.1093/scan/nsm015.

Wagner, H.H., Dray, S., 2015. Generating spatially constrained null models for irregularly spaced data using Moran spectral randomization methods. Methods Ecol. Evol. 6, 1169–1178. doi:10.1111/2041-210X.12407.

Wagstyl, K., Larocque, S., Cucurull, G., Lepage, C., Cohen, J.P., Bludau, S., Palomero-Gallagher, N., Lewis, L.B., Funck, T., Spitzer, H., Dickscheid, T., Fletcher, P.C., Romero, A., Zilles, K., Amunts, K., Bengio, Y., Evans, A.C., 2020. BigBrain 3D atlas of cortical layers: cortical and laminar thickness gradients diverge in sensory and motor cortices. PLoS Biol. 18, e3000678. doi:10.1371/journal.pbio.3000678.

Wang, Y., Royer, J., Park, B., Vos de Wael, R., Lariviere, S., Tavakol, S., Rodriguez-Cruces, R., Paquola, C., 2022. Long-range functional connections mirror and link microarchitectural and cognitive hierarchies in the human brain. Cereb. Cortex in press doi:10.1093/cercor/bhac172.

Whitaker, K.J., Vértes, P.E., Romero-Garcia, R., Váša, F., Moutoussis, M., Prabhu, G., Weiskopf, N., Callaghan, M.F., Wagstyl, K., Rittman, T., Tait, R., Ooi, C., Suckling, J., Inkster, B., Fonagy, P., Dolan, R.J., Jones, P.B., Goodyer, I.M., Consortium, the N., Bullmore, E.T., 2016. Adolescence is associated with genomically patterned consolidation of the hubs of the human brain connectome. Proc. Natl Acad. Sci. 113, 9105–9110. doi:10.1073/pnas.1601745113.

Woo, C.-W., Krishnan, A., Wager, T.D., 2014. Cluster-extent based thresholding in fMRI analyses: Pitfalls and recommendations. Neuroimage 91, 412–419. doi:10.1016/j.neuroimage.2013.12.058.

Worsley, K.J., Taylor, J.E., Carbonell, F., Chung, M., Duerden, E., Bernhardt, B., Lyttelton, O., Boucher, M., Evans, A., 2009. SurfStat: a Matlab toolbox for the statistical analysis of univariate and multivariate surface and volumetric data using linear mixed effects models and random field theory. Neuroimage S102.

Worsley, K.J., Andermann, M., Koulis, T., MacDonald, D., Evans, A.C., 1999. Detecting changes in nonisotropic images. Hum. Brain Mapp. 8 (2-3), 98–101.

Xu, T., Nenning, K.-H., Schwartz, E., Hong, S.-J., Vogelstein, J.T., Goulas, A., Fair, D.A., Schroeder, C.E., Margulies, D.S., Smallwood, J., Milham, M.P., Langs, G., 2020. Cross-species functional alignment reveals evolutionary hierarchy within the connectome. Neuroimage 223, 117346. doi:10.1016/j.neuroimage.2020.117346.

Yarkoni, T., Poldrack, R.A., Nichols, T.E., Van Essen, D.C., Wager, T.D., 2011. Large-scale automated synthesis of human functional neuroimaging data. Nat. Methods 8, 665–670. doi:10.1038/nmeth.1635.

Yeo, B.T.T., Krienen, F.M., Sepulcre, J., Sabuncu, M.R., Lashkari, D., Hollinshead, M., Roffman, J.L., Smoller, J.W., Zöllei, L., Polimeni, J.R., Fischl, B., Liu, H., Buckner, R.L., 2011. The organization of the human cerebral cortex estimated by intrinsic functional connectivity. J. Neurophysiol. 106, 1125–1165. doi:10.1152/jn.00338.2011.